Materials Innovations

HΣXA Publishers

Research Article | Carbon Materials | http://doi.org/10.54738/MI.2022.21201

Theoretical Elucidation of Tuning the Transport Properties of Doped and Co-Doped Graphene Quantum Dots layer with Adsorption of Porphyrin Molecule Using Non-Equilibrium Green Function

Maha Tariq[1], Ambreen Kalsoom[1]*, Misbah Mirza[2], Waseem Akhtar Qureshi[3], Shamroza Mubarik[4], Adnan Mujahid[5], Zahida Batool[6]

1 Department of Physics Govt, Sadiq College Women University Bahawalpur, 63100, Punjab, Pakistan
2 Department of Physics, The Women University Multan, 60000, Multan, Pakistan
3 Cholistan Institute of Desert Studies (CIDS), Baghdad–ul–Jadeed Campus, The Islamia University of Bahawalpur-63100, Pakistan, Bahawalpur, 63100, Pakistan
4 Department of Chemistry, The Govt Sadiq College Women University, 63100, Bahawalpur, Punjab, Pakistan
5 School of Chemistry, University of the Punjab, Lahore, 54590, Pakistan
6 Institute of Physics, The Islamia University of Bahawalpur, Bahawalpur, 63100, Pakistan

OPEN ACCESS

Received: 03 December 2022
Accepted: 17 December 2022
Published: 29 December 2022

Citation: Tariq M, Kalsoom A, Mirza M, Qureshi WA, Mubarik S, Mujahid A, Batool Z (**2022**) Theoretical Elucidation of Tuning the Transport Properties of Doped and Co-Doped Graphene Quantum Dots layer with Adsorption of Porphyrin Molecule Using Non-Equilibrium Green Function. *Materials Innovations 2* (12), 317-325.

***Correspondence**: (Ambreen Kalsoom) kalsoom.ambreen@gscwu.edu.pk,

Published By Hexa Publishers

ISSN
Electronic: 2790-1963

Theoretical elucidation of tuning the transport properties of nitrogen and boron doped and co-doped single layer graphene quantum dots with adsorbed porphyrin molecule by using non-equilibrium Green's function and ab initio method was investigated. The impacts of doping, co-doping of nitrogen, boron atoms on transport properties such as density of state (DOS), transmission coefficient (TE) and current voltage characteristics is demonstrated. Results showed that the adsorption of porphyrin molecule on un-doped GQDs layer increases the conductivity of GQDs layer. Moreover, the conductance mechanism of the devices in case of doping of boron and co-doping of nitrogen, boron in GQDs layer with adsorbed porphyrin molecule may initially increases at the same rate but slightly lesser than un-doped GQDs layer with adsorbed porphyrin molecule. It may be noted, that doping of nitrogen in GQDs layer reduces the conductance drastically. Finally, we have concluded that adsorbed porphyrin molecule interacts strongly with un-doped GQDs layer. Theoretical studies suggested that we can use these graphene quantum dots-based devices as a chemical sensor or as a switching device.

Keywords: Transport properties, Porphyrin molecule, Graphene quantum dots, Doped graphene quantum dots, Nitrogen doping, Boron doping, Co-doping

INTRODUCTION

Isolation of single layer from graphite has started new era of graphene and related two-dimensional materials[1,2]. Graphene is a single atomic layer that is firmly packed into a two-dimensional (2D) honeycomb lattice[3–8]. Graphene is the fundamental component of all the graphitic materials, including

zero-dimensional (0D) fullerenes, one-dimensional (1D) nanotubes, and three-dimensional (3D) graphite, which are created by cutting, wrapping, rolling, and stacking graphene, respectively. Due to its promising applications, graphene has become an attractive material for theoretical and experimental studies[9,10 11]. Graphene-based materials have drawn a lot of interest because of their exceptional chemical, mechanical, electrical, and optical capabilities[12 13]. Due to the desire to make electronic gadgets smaller and more powerful, new materials are continuously being developed. A complex made of carbon and boron atoms is a logical progression in the research of graphene. Due to its nearly identical atomic radius, the substitution of boron for carbon in graphene is rational choice. Researchers predicted that boron carbon graphene would have properties similar to carbon graphene in the field of electronic devices[14]. By reducing the dimension of graphene, graphene nanoribbons (GNRs) and graphene quantum dots (GQDs) have been fabricated[3]. Carbon-based fluorescent nanostructures known as graphene quantum dots (GQDs) have a wide range of uses because of their fascinating characteristics. Applications of GQDs are limited due to their low photoluminescence (PL) yield and monochromatic PL behavior. As a result, it is acknowledged that heteroatom (nitrogen, boron) doping of GQDs is the best method for changing the optical and electrical and transport properties of GQDs[15]. The interaction between the surface dopants and the adsorbents is maximized in GDDs, which is thought to be a superior sensor material[16]. In today's integrated circuits, dopant atoms are significant[17]. Doping, is the one of the fundamental processes in electronics; it is the process of introducing specific chemical components to a sensor device in order to modify its electrochemical properties. Doping, involves chemically replacing carbon atoms in sp^2-bonded carbon networks with neutral elements is one of the most promising methods for modifying the electrical characteristics of graphene[18–23]. Improvement of intrinsic properties like chemical stability and conductivity can be achieved by doping graphene quantum dots (GQDs) with heteroatoms like nitrogen (N) and boron (B)[24–26]. Chemically doped graphene quantum dot has many novel properties. In comparison to undoped GQDs, it was claimed that B and N-doped GQDs displayed excellent specific capacities in lithium and sodium ions batteries. N-doped GQDs increase the active sites on their surface, making them a superior luminescent material and effective catalysts[27]. Because of their dependable and predictable electrical properties, boron doped (B-doped) GQDs can be used in a variety of applications, including electrocatalysis and nanoelectronics[18]. Adsorption is the process by which a material or molecule called an adsorbent contracted on the surface of an absorbent. One of the fundamental steps in the fabrication of molecular-based nanodevices is the adsorption of complex molecules on solid surfaces. The physical and chemical properties of adsorbed molecules are determined by their geometric structure and arrangement, making molecular scale determination and control processes particularly appealing[28–30]. Charge transfer and charge recombination at the molecule/semiconductor interface, as well as the overall efficiency may be limited by the molecule tethering mechanism and adsorption geometry[31–35]. Herein, we focused on the adsorption structure of the porphyrin molecule and its ordering on a graphene quantum dot layer. Porphyrin and their metallic derivatives can be synthesized using a variety of techniques that have been extensively researched in the scientific literature[36–39]. Porphyrins may be used in functional materials, sensors, catalysts, and other products. These versatile materials are highly helpful in a variety of processes, including catalytic and photocatalytic ones[37]. In this paper, we have studied the impact of doping, co-doping of nitrogen, boron on transport properties of single layer of GQD and with adsorption of porphyrin molecule onto these GQD layers.

CALACULATION METHODS

Doping, co-doping of nitrogen (N), boron (B) and adsorbed porphyrin molecule with GQDs layer (signified as GQDs, N-GQDs, B-GQDs, NB-GQDs, GQDs@porphyrin, N-GQDs@porphyrin, B-GQDs@porphyrin, NB-GQDs@porphyrin) were completely optimized using B3LYP/6-31G as performed in Gauss view 5.0. The geometry of the device consisted of 80 atoms in total, out of which there were 48 carbon atoms, 26 hydrogen atoms, 4 nitrogen atoms and 2 sulfur atoms. The edge atoms have been passivated with hydrogen atoms. After optimization the doping and co-doping sites of nitrogen and boron in GQDs are different from adsorption of porphyrin molecule onto GQDs. The gaussian calculation found that the adsorption energy of GQDs@porphyrin is -0.113eV, N-GQDs@porphyrin is -0.0016 eV, B-GQDs@porphyrin is -0.0020 eV and NB-GQDs@porphyrin is 0.0014 eV respectively. The adsorption energy (E_{ad}) calculated using Eq. (1).

$$E_{ad} = E_{tot}(E_{tot}(X-doped.GQDs) - E_{tot}(porphyrin) \quad (1)$$

In Eq. (1) X can either be Boron, Nitrogen or both NB, and E_{tot}(GQDs@porphyrin) is the total energy of porphyrin molecule adsorbed on GQDs layer. Where E_{tot}(X-doped. GQDs), E_{tot}(porphyrin) are the total energies doped on graphene quantum dot layer and a porphyrin molecule respectively. It should be noted, that the negative value of E_{ad} varies to exothermic adsorption[11]. The gold electrodes connected with the graphene

quantum dot layer through sulfur atoms and the porphyrin molecule adsorbed on it to create a metal junction structure. The device was split into two parts: an "extended scattering" region comprised of sulfur (S) and GQDs@porphyrin molecules as well as a portion of the metallic electrodes (as in Figure 2). The bond length used here were C-C 1.410 Å, C-H 1.085 Å, Au-Au 2.885 Å, S-Au 2.530 Å and S-C 1.730 Å respectively. The nitrogen and boron locate with the bond length of C-B 1.426 Å, N-C 1.376 Å in the GQDs layer. The porphyrin molecule locates at the length 4.217 Å form the GQDs surface. The non-equilibrium method was used to study the transmission function for single GQDs layer and GQDs@porphyrin systems. Utilizing the non-equilibrium Green's functional approach with a tight-binding Hamiltonian in Eq. 2.[40].

$$T = Tr(\Gamma_1 G \Gamma_2 G^+) \quad (2)$$

G(G^+) stands for the advance green function, The coupling between the electrodes with the numbers 1 and 2 is described by $\Gamma_{1,2}$ respectively, and is exclusively given by the imaginary part of the electrode's self-energy. Terminal current is[40].

$$I = \frac{2e}{h}\int_{-\infty}^{+\infty} dET\ (E, V) \times [f\ (E, \mu_1) - f\ (E, \mu_2)] \quad (3)$$

$\mu_{1(2)} = E_F \pm \frac{eV}{2}$

Where $\mu_{1(2)}$ the electrochemical potentials of the left and right electrodes, and E_f is the Fermi function. The Hückel-IV program with code created at Purdue University was utilized to calculate the transport properties of graphene quantum dot devices with adsorbed porphyrin molecule. This program connected the molecule to the electrodes using a three-atom Au pads (consisting of three, seven or three gold layers as in Figure 1). The Fermi level in the GQDs-based devices is -11.8 eV, as based on earlier research[41].

RESULTS AND DISCUSSION

The optimized structures of doped, co-doped graphene quantum dots layer sandwiched between Au electrodes are represented in Figure 1.

In Figure 2, the optimized structure of un-doped GQDs@porphyrin molecule is illustrated. It shows scattering region with the configuration of 13 gold electrodes attached on left and right side with graphene quantum dots layer. Optimized configuration of adsorbed porphyrin molecule onto graphene quantum dots layers investigated in this work is represented in Figure 3. The detail on density of states (DOS) of the GQDs layers and with adsorption of porphyrin molecule onto these GQDs layers around Fermi level are presented in Figure 4. It can be seen that there are some differences: Firstly, for each of the eight structures, there are distinct differences in the DOS peaks, positions and heights. Secondly, in DOS Fermi level has distinct numbers of peaks, and the spaces between those peaks are also different from one another. The device displays metallic characteristics because the total DOS was not zero near the Fermi level. From Figure 4 it can be seen that GDQs have more resonance peaks and height of resonance peaks are largest for the range of -12 to -14eV. While for N-GQDs and NB-GQDs almost similar smaller peaks are observed expect for the short range of -8 and to -9.5eV. While for B-GQDs gap between resonance peaks are greatest which ensures the availability of less energy levels for B-GQDs (as in Figure 4A). Now we discussed the cases, when we have absorbed porphyrin molecule onto these GQDs layers. We have seen that GQDs@porphyrin device has more resonance peaks and the gap of resonance peaks are small which ensure that more energy levels are available in GQDs@porphyrin. In GQDs@porphyrin two distinct resonance peaks above and below the Fermi energy were seen. This might have happened as a result of the stronger degree of hybridization between GQDs and adsorbed porphyrin molecule. The GQDs@porphyrin molecule has internal charges that were redistributed as a result of the applied voltage, which had an impact on the charge transport characteristics.

In the DOS spectrum, there were no significant changes for B-GQDs@porphyrin, NB-GQDs@porphyrin in the energy range between -12 and -14 eV. However, for N-GQDs@porphyrin less resonance peaks are observed for the same range (-12 to -14 eV). For the case N-GQDs@porphyrin, NB-GQDs@porphyrin nearly identical and small resonance peaks are found for the energy range between -6 eV to -11 eV which has minimal effect on conductance capability. Moreover, the strength of resonance peaks is small for the case of NB-GQDs@porphyrin. For B-GQDs and B-GQDs@porphyrin showed prominent conductance effect but slightly lesser as compared to GQDs and GQDs@porphyrin. Therefore, it is concluded that GQDs and GQDs@porphyrin has significant effect on conductance capacity whereas, doping of nitrogen and co-doping of nitrogen, boron demonstrates minimal effect on single layer of GQDs and GQDs@porphyrin.

In Figure 5, the transmission coefficient for all structures is presented. Peaks in the transmission coefficients are well correlated with those in the peaks of DOS in terms of their positions. However, the height of the transmission peak is not exactly mapped onto the height of the DOS peaks. Strength of resonance peaks intensities in structure of GQDs were greater as compared to N-GQDs, B-GQDs, NB- GQDs. However it should be noted that height of peaks become wider after adsorption of porphyrin molecule onto these GQDs layers (as in Figure 5). Stronger resonance peaks have been seen for the case of GQDs@porphyrin. At a moderate

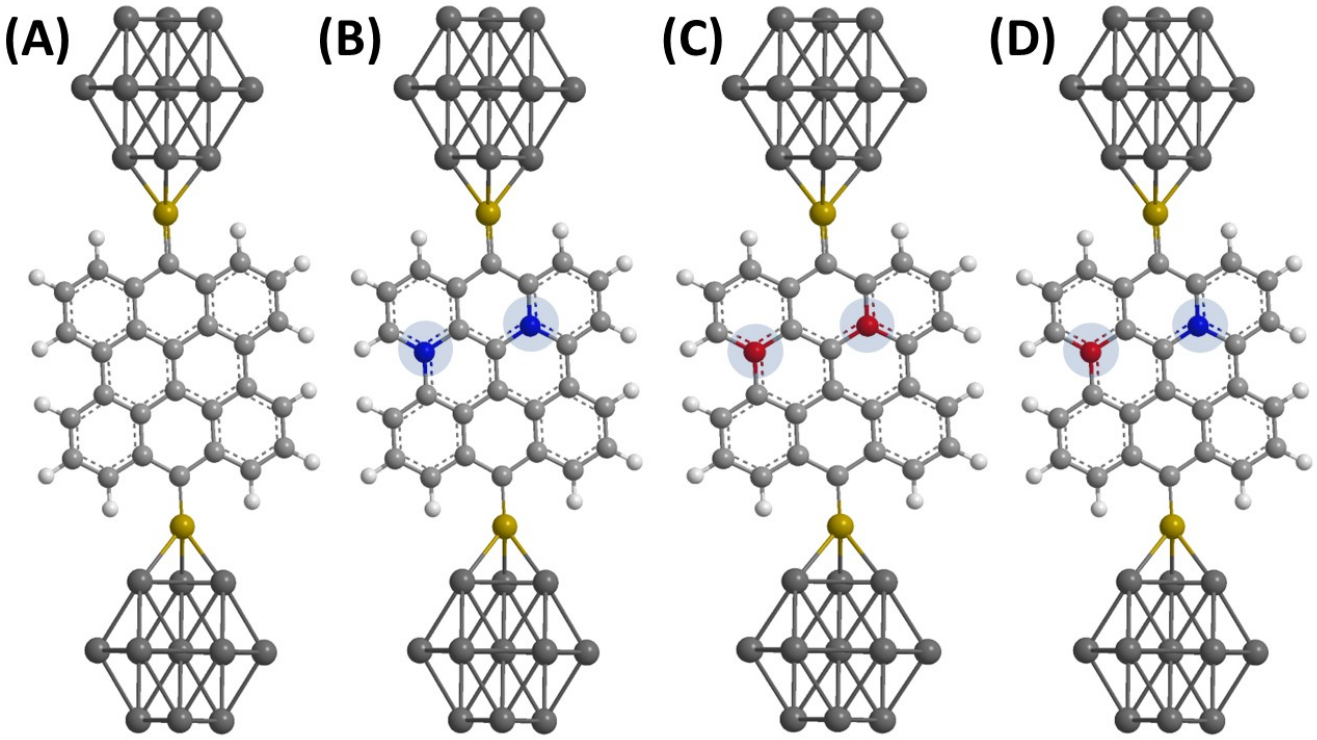

Figure 1. Optimized structures of GQDs devices demonstrated in this work. (A) represent un-doped GQDs, (B) represent N-GQDs, (C) represent B-GQDs and (D) represent NB-GQDs. (Highlighted portion presents doping and co-doping, blue color is for nitrogen and red color is for boron atoms)

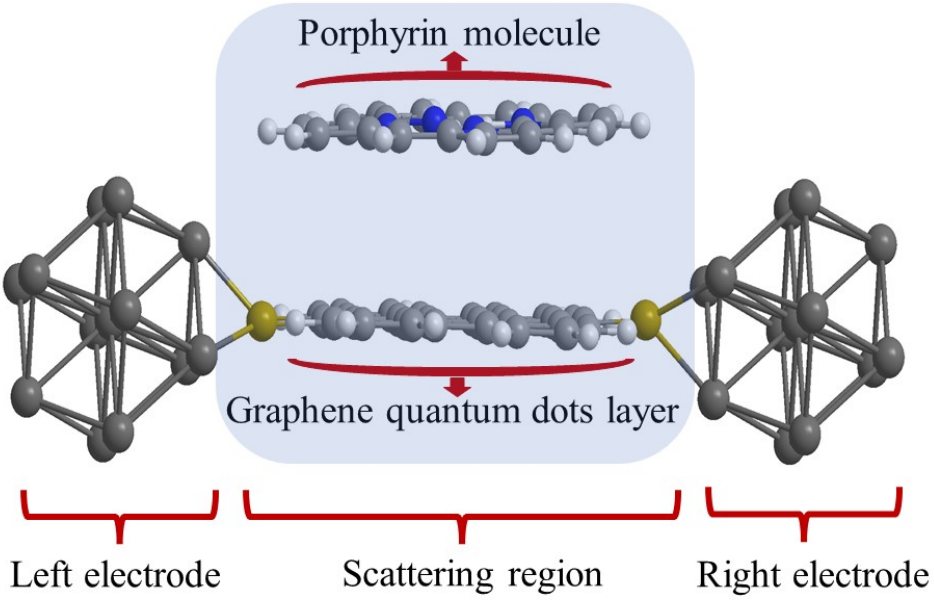

Figure 2. Horizontal view of optimized structure of GQDs@porphyrin molecule. The edge atom has been passivated with hydrogen atoms.

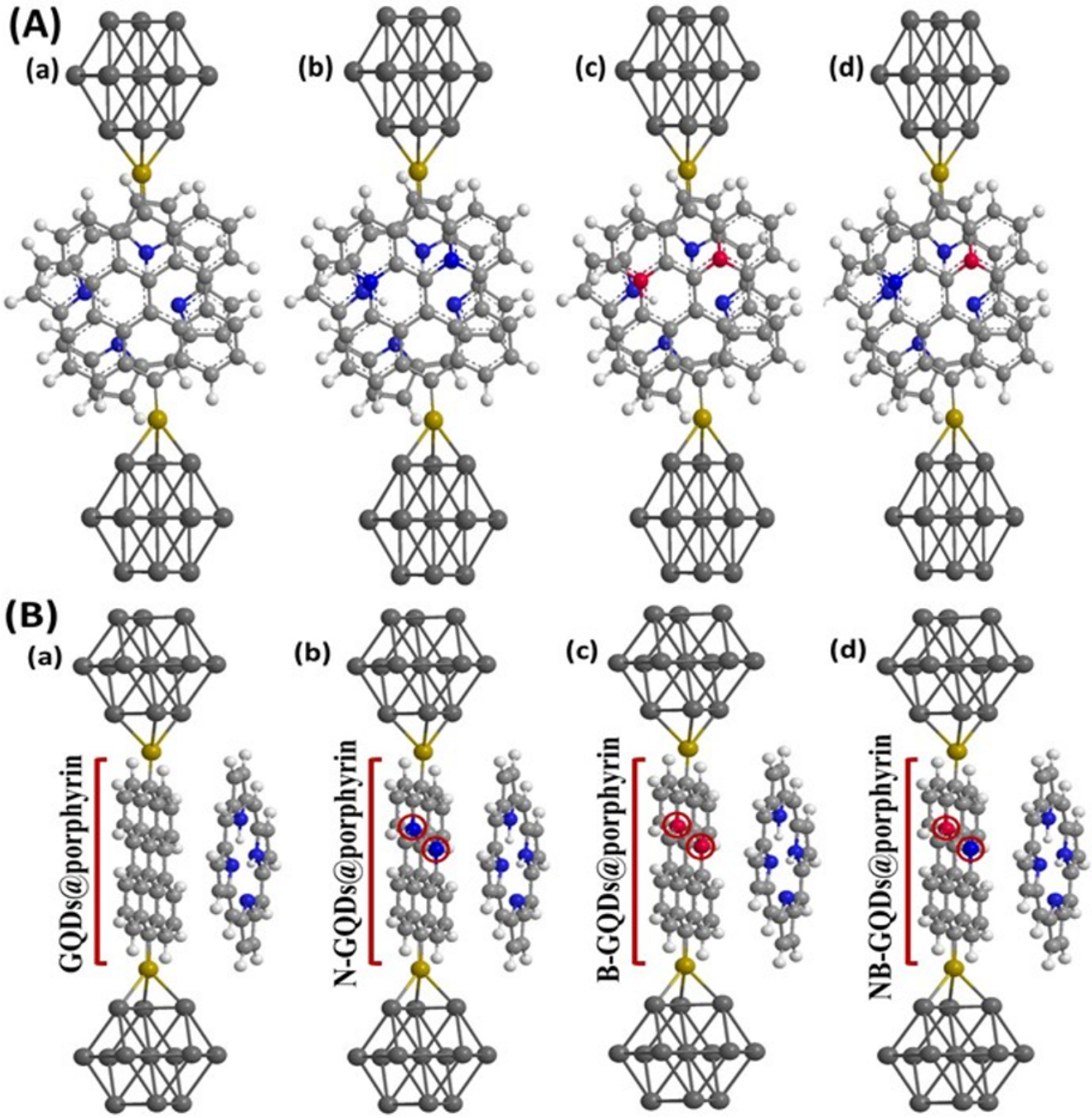

Figure 3. Structural representation of optimized devices investigated in this work: Fig. 2A (a, b, c, d) represent front view whereas, 2B (a, b, c, d) represent side view of GQDs@porphyrin, N-GQDs@porphyrin, B-GQDs@porphyrin and NB-GQDs@porphyrin molecule.

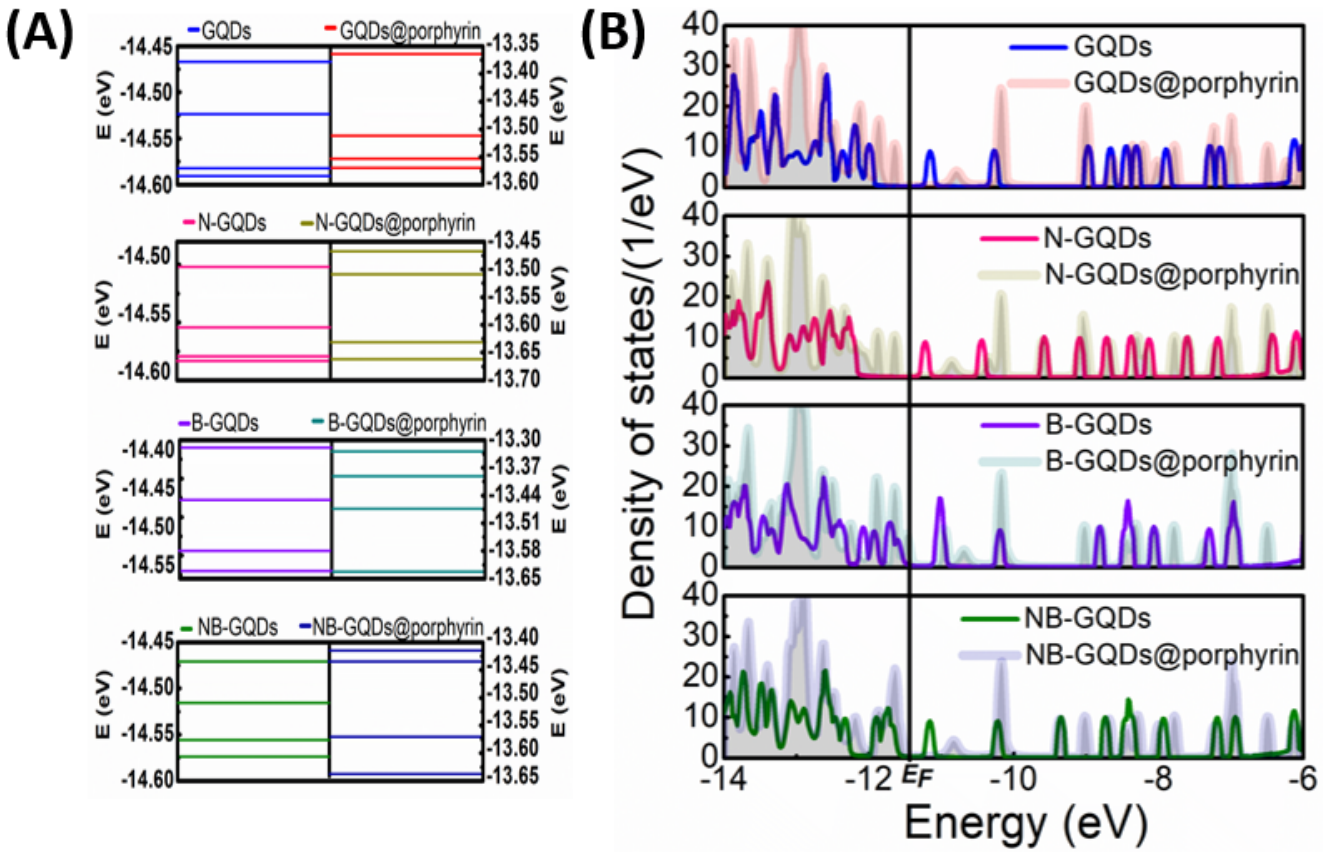

Figure 4. (A) display energy levels and (B) presented the total densities of states for graphene quantum dots layer (GQDs, N-GQDs, B-GQDs, NB-GQDs) and graphene quantum dots layer with adsorption of porphyrin molecule (GQDs@porphyrin, N-GQDs@porphyrin, B-GQDs@porphyrin, NB-GQDs@porphyrin).

bias, a significantly larger current is expected in GQDs@porphyrin. Noted, that the terminal current is determined by using Eq. (3) is proportional to the transmission coefficient integral over the bias window around the E_F .

We can observe that in intensities of peaks in transmission co-efficient for GQDs@porphyrin are higher than those of others especially for the range of -14 to -11eV. Results showed that amplitude of transmission co-efficient decreasing by doping (N-GQDs@porphyrin, B-GQDs@porphyrin) but almost negligible by co-doping (NB-GQDs@porphyrin). The I-V characteristics of GQDs, GQDs@porphyrin, N-GQDs, N-GQDs@porphyrin, B-GQDs, B-GQDs@porphyrin NB-GQDs and NB-GQDs@porphyrin devices were calculated over a bias voltage ranging from 0 to 4V, as presented in Figure 6.

The current in case of GQDs and B-GQDs almost increases in the same manner also for NB-GQDs current increases initially but decreases after 2V. But for N-GQDs almost negligible current have been observed. The behavior of current for the case of GQDs@porphyrin and B-GQDs@porphyrin are pretty close to each other. Also current in NB- GQDs@porphyrin is initially increased in the same manner but slightly decreased as compared to GQDs@porphyrin and B-GQDs@porphyrin as shown in Figure 6. Therefore, the current in GQDs@porphyrin was high as compared to all structures. In contrast the I-V of the N-GQDs@porphyrin is considerably low bias and increase nonlinearly with bias. This process suggested that the barrier electron transport of the devices with GQDs@porphyrin, B-GQDs@porphyrin and NB-GQDs@porphyrin structure are reduced and current-carrying capabilities are enhanced as compared to N-GQDs@porphyrin one. Therefore, it is concluded that un-doped graphene quantum dots layer interacts strongly with adsorbed porphyrin molecule as compared to other, while N-GQDs@porphyrin molecule provide higher barrier for charge as a result of which this structure shows lower transmission probability. Consequently, the current has almost no effect when we doped nitrogen in GQDs layer. It should be obvi-

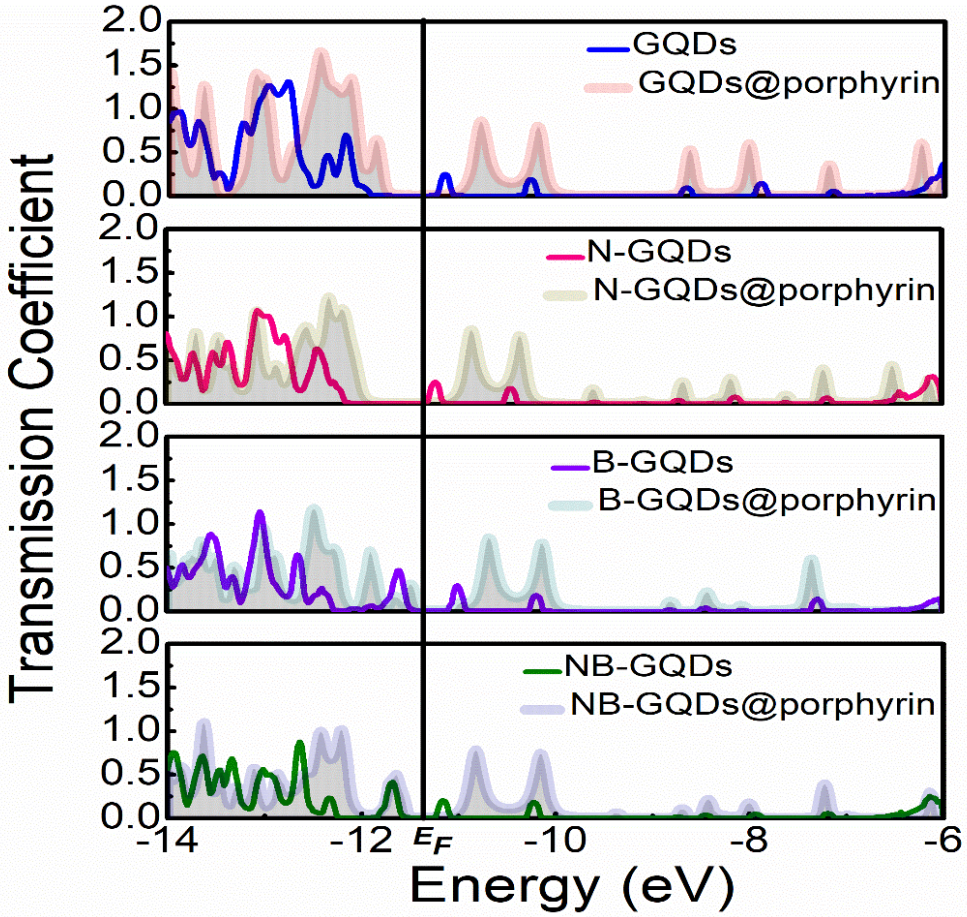

Figure 5. Total transmission coefficient of all the structures: GQDs, N-GQDs, B-GQDs, NB-GQDs, GQD@porphyrin, N-GQD@porphyrin, B- GQD@porphyrin and NB-GQD@porphyrin are presented.

ous that the adsorption of porphyrin molecule onto un-doped graphene quantum dots layer shows higher conducting capabilities as compared to the other devices (N-GQDs@porphyrin, B- GQDs@porphyrin and NB-GQDs@porphyrin).

CONCLUSIONS

In this work, we have theoretically investigated transport properties of doped and co-doped graphene quantum dots layer and GQDs with adsorbed porphyrin molecule by using the non-equilibrium Green's function approach. The estimations made use of a tight-binding Hamiltonian. The results showed that the transport properties of single layer of graphene quantum dots and with adsorbed porphyrin molecule can be easily tuned. Findings indicates that doping of nitrogen in single graphene quantum dots layer has no significant effect on conductance capability as compared to un-doped and boron doped GQDs layer. It should be concluded that porphyrin molecule interacts strongly with un-doped graphene quantum dots layer. Therefore, larger current and more energy level available for un-doped graphene quantum dots layer with adsorbed porphyrin molecule. However, the transmission coefficient shows that, a significantly larger current is expected in GQDs@porphyrin. Moreover, for the case of adsorbed porphyrin molecule, doping of nitrogen in GQDs layer reduces the current drastically. Therefore, the current has almost no effect when we doped nitrogen in GQDs layer. The effect of size of un-doped, nitrogen and boron doped and also co-doping of nitrogen and boron in graphene quantum dots layer is evident. However, doping and co-doping in graphene quantum dots layer with adsorbed porphyrin molecule significantly alters the transport properties and conductance of GQDs layer. Making nano size electrical devices like quantum dot gas sensors requires knowledge of how the transport char-

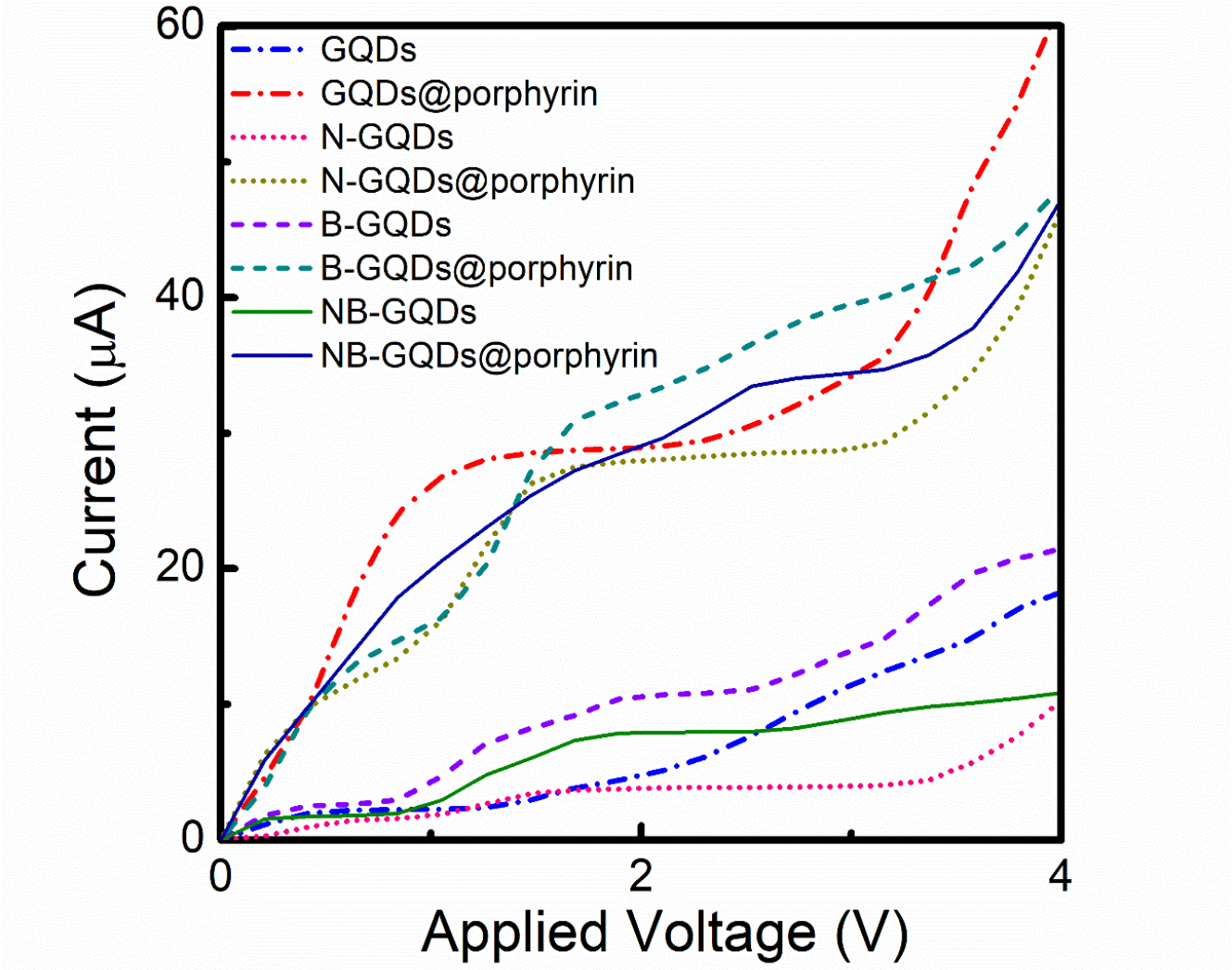

Figure 6. Current-voltage characteristics for the all types of structures investigated (GQDs, N-GQDs, B-GQDs, NB-GQDs, GQDs@porphyrin, N-GQDs@porphyrin, B-GQDs@porphyrin and NB-GQDs@porphyrin).

acteristics vary as a porphyrin molecule is adsorbed in various configurations.

References

1) Geim, A. K. Graphene: status and prospects. *Science* **2009**, *324* (5934), 1530–1534.
2) Xinming, L.; Tao, L.; Chen, Z.; Fang, H.; Li, X.; Wang, X.; Xu, J.-B.; Zhu, H.; Hongwei Zhu, Graphene and related two-dimensional materials: Structure-property relationships for electronics and optoelectronics. *Applied Physics Reviews* **2017**, *4* (2), 021306.
3) Wang, F. Tuning properties of NC3H quantum dot by adsorption of ammonia and carbon dioxide. *Current Applied Physics* **2015**, *15* (11), 1348–1352.
4) Oliveira, A. M. L.; Machado, M.; Silva, G. A.; Bitoque, D. B.; Ferreira, J. T.; Pinto, L. A.; Ferreira, Q. Graphene Oxide Thin Films with Drug Delivery Function. *Nanomaterials 12* (7), 1149–1149.
5) Razaq, A.; Bibi, F.; Zheng, X.; Papadakis, R.; Jafri, S. H. M.; Li, H. Review on Graphene-, Graphene Oxide-, Reduced Graphene Oxide-Based Flexible Composites: From Fabrication to Applications. *Materials 15* (3), 1012–1012.
6) Kaewmaraya, T.; Ngamwongwan, L.; Moontragoon, P.; Jarernboon, W.; Singh, D.; Ahuja, R.; Karton, A.; Hussain, T. Novel green phosphorene as a superior chemical gas sensing material. *Journal of Hazardous Materials* **2021**, *401*, 123340–123340.
7) Khan, Z. U.; Kausar, A.; Ullah, H.; Badshah, A.; Khan, W. U. A review of graphene oxide, graphene buckypaper, and polymer/graphene composites: Properties and

fabrication techniques. *Journal of Plastic Film & Sheeting* **2016**, *32* (4), 336–379.
8) Geim, A. K.; Novoselov, K. S. The rise of graphene. *Nanoscience and Technology* **2009**, *6*, 11–19.
9) Xu, Y.; Ali, A.; Shehzad, K.; Meng, N.; Xu, M.; Zhang, Y.; Wang, X.; Jin, C.; Wang, H.; Guo, Y.; Yang, Z.; Yu, B.; Liu, Y.; He, Q.; Duan, X.; Wang, X.; Tan, P.-H.; Hu, W.; Lu, H.; Hasan, T. Solvent-Based Soft-Patterning of Graphene Lateral Heterostructures for Broadband High-Speed Metal–Semiconductor–Metal Photodetectors. *Advanced Materials Technologies* **2017**, *2* (2), 1600241.
10) Chen, X.; Shehzad, K.; Gao, L.; Long, M.; Guo, H.; Qin, S.; Wang, X.; Wang, F.; Shi, Y.; Hu, W.; Xu, Y.; Wang, X. Graphene hybrid structures for integrated and flexible optoelectronics. *Advanced Materials* **2020**, *32* (27), 1902039.
11) Seyed-Talebi, S. M.; Beheshtian, J.; Neek-Amal, M. Doping effect on the adsorption of NH₃ molecule onto graphene quantum dot: From the physisorption to the chemisorption. *Journal of Applied Physics* **2013**, *114* (12), 124307–124307.
12) Soldano, C.; Mahmood, A.; Dujardin, E. Production, properties and potential of graphene. *Carbon* **2010**, *48* (8), 2127–2150.
13) Malček, M.; Müllerová, S.; Bučinský, L. Theoretical study of hydrogen adsorption on the graphene quantum dots doped with various first row transition metals: Switch of spin state as a way to improve H2 adsorption. *Physica E: Low-dimensional Systems and Nanostructures* **2022**, *139*, 115144–115144.
14) Li, G.; Li, R. The transport properties of the molecular-scale B2C and BC3 electronic devices. *Physica B: Condensed Matter* **2012**, *407* (17), 3419–3422.
15) Sohal, N.; Maity, B.; Basu, S. Recent advances in heteroatom-doped graphene quantum dots for sensing applications. *RSC Advances* **2021**, *11* (41), 25586–25615.
16) Zhang, Z.; Zhang, X.; Luo, W.; Yang, H.; He, Y.; Liu, Y.; Zhang, X.; Peng, G. Study on adsorption and desorption of ammonia on graphene. *Nanoscale Research Letters* **2015**, *10* (1), 1–8.
17) Zhang, C.; Chang, S.; Dan, Y. Advances in ultrashallow doping of silicon. *Advances in Physics: X* **2021**, *6* (1), 1871407–1871407.
18) Yeom, D.-Y.; Jeon, W.; Tu, N. D. K.; Yeo, S. Y.; Lee, S.-S.; Sung, B. J.; Chang, H.; Lim, J. A.; Kim, H. High-concentration boron doping of graphene nanoplatelets by simple thermal annealing and their supercapacitive properties. *Scientific Reports* **2015**, *5* (1), 1–10.
19) Zhang, Y.; Ge, J.; Wang, L.; Wang, D.; Ding, F.; Tao, X.; Chen, W. Manageable N-doped Graphene for High Performance Oxygen Reduction Reaction. *Scientific Reports* **2013**, *3* (1), 1–8.
20) Liu, H.; Liu, Y.; Zhu, D. Chemical doping of graphene. *J. Mater. Chem.* **2011**, *21* (10), 3335–3345.
21) Panchakarla, L. S.; Subrahmanyam, K. S.; Saha, S. K.; Govindaraj, A.; Krishnamurthy, H. R.; Waghmare, U. V.; Rao, C. N. R. Synthesis, Structure, and Properties of Boron- and Nitrogen-Doped Graphene. *Advanced Materials* **2009**, *21* (46), NA–NA.
22) Wei, D.; Liu, Y.; Wang, Y.; Zhang, H.; Huang, L.; Yu, G. Synthesis of N-Doped Graphene by Chemical Vapor Deposition and Its Electrical Properties. *Nano Letters* **2009**, *9* (5), 1752–1758.
23) Blackburn, J. L.; Yan, Y.; Engtrakul, C.; Parilla, P. A.; Jones, K.; Gennett, T.; Dillon, A. C.; Heben, M. J. Synthesis and Characterization of Boron-Doped Single-Wall Carbon Nanotubes Produced by the Laser Vaporization Technique. *Chemistry of Materials* **2006**, *18* (10), 2558–2566.
24) Adel, R.; Ebrahim, S.; Shokry, A.; Soliman, M.; Khalil, M. Nanocomposite of CuInS/ZnS and Nitrogen-Doped Graphene Quantum Dots for Cholesterol Sensing. *ACS Omega* **2021**, *6* (3), 2167–2176.
25) Zhu, S.; Song, Y.; Zhao, X.; Shao, J.; Zhang, J.; Yang, B. The photoluminescence mechanism in carbon dots (graphene quantum dots, carbon nanodots, and polymer dots): current state and future perspective. *Nano Research* **2015**, *8* (2), 355–381.
26) Qu, D.; Zheng, M.; Du, P.; Zhou, Y.; Zhang, L.; Li, D.; Tan, H.; Zhao, Z.; Xie, Z.; Sun, Z. Highly luminescent S, N co-doped graphene quantum dots with broad visible absorption bands for visible light photocatalysts. *Nanoscale* **2013**, *5* (24), 12272–12272.
27) Li, Y.; Wu, F.; Jin, X.; Xu, H.; Liu, X.; Shi, G. Preparation and electrochemical properties of graphene quantum dots/biomass activated carbon electrodes. *Inorganic Chemistry Communications* **2020**, *112*, 107718–107718.
28) Yokoyama, T.; Yokoyama, S.; Kamikado, T.; Mashiko, S. Nonplanar adsorption and orientational ordering of porphyrin molecules on Au(111). *The Journal of Chemical Physics* **2001**, *115* (8), 3814–3818.
29) Gimzewski, J. K.; Joachim, C.; Schlittler, R. R.; Langlais, V.; Tang, H.; Johannsen, I. Rotation of a Single Molecule Within a Supramolecular Bearing. *Science* **1998**, *281* (5376), 531–533.
30) Jung, T. A.; Schlittler, R. R.; Gimzewski, J. K. Conformational identification of individual adsorbed molecules with the STM. *Nature* **1997**, *386* (6626), 696–698.
31) Fernández, C. C. Adsorption of phosphonic-acid-functionalized porphyrin molecules on TiO2 (110). *The Journal of Physical Chemistry C* **2019**, *123*, 10974–10980.
32) Clifford, J. N.; Palomares, E.; Nazeeruddin, M. K.; Grätzel, M.; Nelson, J.; Li, X.; Long, N. J.; Durrant, J. R. Molecular Control of Recombination Dynamics in Dye-Sensitized Nanocrystalline TiO₂ Films: Free Energy vs Distance Dependence. *Journal of the American Chemical Society* **2004**, *126* (16), 5225–5233.
33) Clifford, J. N. Molecular control of recombination dynamics in dye sensitised nanocrystalline TiO 2 films. *Chemical Communications* **2002**, (12), 1260–1261.
34) Ladomenou, K.; Kitsopoulos, T. N.; Sharma, G. D.; Coutsolelos, A. G. The importance of various anchoring groups attached on porphyrins as potential dyes for DSSC applications. *RSC Adv.* **2014**, *4* (41), 21379–21404.
35) Hart, A. S.; Kc, C. B.; Gobeze, H. B.; Sequeira, L. R.; D'souza, F. Porphyrin-Sensitized Solar Cells: Effect of Carboxyl Anchor Group Orientation on the Cell Performance. *ACS Applied Materials & Interfaces* **2013**, *5* (11), 5314–5323.
36) Samia, A.; Feddi, E.; Duque, C. A.; Mora-Ramos, M. E.; Akimov, V.; Correa, J. D. Optoelectronic properties of phosphorene quantum dots functionalized with free base porphyrins. *Computational Materials Science* **2020**, *171*, 109278–109278.
37) Faraon, V. A.; Pop, S. F.; Senin, R. M.; Doncea, S. M.; Ion, R. M. Porphyrin-zeolite nanomaterials for hydrogen peroxide decomposition. *SPIE Proceedings* **2012**,
38) Richardson, C.; Reed, C. A. Synthesis of meso-extended tetraarylporphyrins. *The Journal of organic chemistry* **2007**, *72*, 4750–4755.
39) Marsh, D. F.; Falvo, R. E.; Mink, L. M. Microscale Synthesis and 1H NMR Analysis of Tetraphenylporphyrins. *Journal of Chemical Education* **1999**, *76* (2), 237–237.
40) Datta, S. In *Electronic Transport in Mesoscopic Systems*; and others„ Ed.; Cambridge University Press, 1995.
41) Song, S.; Li, G. Current shot noise characteristics in biphenyl diamine and biphenyl dithiol devices. *Applied Physics A* **2014**, *116* (3), 1489–1493.